Tamaki, K., Suyehiro, K., Allan, J., McWilliams, M., et al., 1992
Proceedings of the Ocean Drilling Program, Scientific Results, Vol. 127/128, Pt. 2

50. ^{40}Ar-^{39}Ar ANALYSIS OF VOLCANIC ROCKS RECOVERED FROM THE JAPAN SEA FLOOR: CONSTRAINTS ON THE AGE OF FORMATION OF THE JAPAN SEA[1]

Ichiro Kaneoka,[2] Yutaka Takigami,[3] Nobuo Takaoka,[4] Shigeru Yamashita,[2] and Kensaku Tamaki[5]

ABSTRACT

Volcanic rocks recovered from the Japan Sea during ODP Legs 127 and 128 were analyzed by ^{40}Ar-^{39}Ar whole-rock stepwise-heating experiments. All three experiments on samples from Site 795 in the Japan Basin revealed disturbed age spectra, but they are consistent with crystallization ages of 15 to 25 Ma for the samples. At Site 797 in the Yamato Basin, three of the five samples showed plateau ages of 18–19 Ma. At Site 794 in the northern Yamato Basin, three of the five samples revealed concordant age spectra of 20–21 Ma. The radiometric age results are consistent with the estimated ages for the oldest sediments at Site 797 based on the biostratigraphy, but are significantly older than those of the oldest sediments at Site 794. However, the radiometric ages are concordant with previously inferred ages for the formation of the Japan Sea floor based on radiometric age data from dredged igneous rocks from the Japan Sea. The present results indicate that formation of the Japan Sea floor started at least 19–20 Ma ago and give more precise age constraints.

INTRODUCTION

Basement volcanic rocks from the Japan Sea floor were recovered by drilling on Ocean Drilling Program (ODP) Legs 127 and 128 (Tamaki, Pisciotto, Allan, et al., 1990; Ingle, Suyehiro, von Breymann, et al., 1990). Numerous arguments have been made about the formation age of the Japan Sea floor based on various approaches, such as stratigraphy, depth of the ocean floor, heat-flow data, geomagnetic lineation pattern, and radiometric age data for rocks dredged from seamounts. Estimated ages range from 10 to 50 Ma (e.g., Lallemand and Jolivet, 1985; Otofuji et al., 1985; Isezaki, 1986; Tamaki, 1986; Kaneoka et al., 1990). However, the most direct method to determine the age of the ocean floor is radiometric dating of basement volcanic rocks cored from the ocean floor. As discussed previously (Kaneoka, 1986), K-Ar ages of submarine volcanic rocks commonly show erroneous values for the age of formation as a result of the occurrence of excess ^{40}Ar and/or post-crystallization ^{40}Ar loss and K addition by the alteration of rocks by seawater. The ^{40}Ar-^{39}Ar method is known as the most suitable for overcoming such problems in dating submarine volcanic rocks.

In this study, we performed ^{40}Ar-^{39}Ar analyses on 13 rock samples recovered from the Japan Sea floor during Legs 127 and 128 with the expectation of determining more precise constraints on the formation age of the Japan Sea floor.

SAMPLES

Basement volcanic rocks were recovered from Sites 794 and 797 in the Yamato Basin and from Site 795 in the Japan Basin (Fig. 1). In order to obtain age information on the evolution of the Japan Sea floor, we selected the most suitable samples for ^{40}Ar-^{39}Ar dating from the available drilled cores. The following criteria were adopted in selecting samples:

1. samples should be as fresh as possible, as determined petrographically;
2. samples should not contain giant phenocrysts and significant amounts of glassy parts (i.e., more than 30%–40%) to minimize the possible occurrence of excess ^{40}Ar (Kaneoka, 1986);
3. samples should cover the wide range of drilled volcanic material in space and time;
4. if sample availability is limited, representative samples from the early stage of evolution should be selected;
5. K content must be reasonably abundant (i.e., more than about 0.2%) to date a volcanic rock of about 10–20 Ma by the ^{40}Ar-^{39}Ar method for the present experiment's conditions.

The freshness of a sample was judged based on the degree of alteration of primary constituent minerals and mesostasis, including the occurrence of secondary minerals.

Based on such criteria, we examined 50 core samples in thin section, from which 18 samples were selected for irradiation with a fast neutron flux for ^{40}Ar-^{39}Ar dating. After irradiation, we found that some samples had a low K content (less than 0.2%) and they were not analyzed further. Hence, a total of 13 samples was analyzed for Ar isotopes (Site 794, 5 samples; Site 795, 3 samples; Site 797, 5 samples). Samples from Sites 797 and 794 represent the seafloor of the Yamato Basin, whereas the samples from Site 795 are from the margin of the Japan Basin (Tamaki, Pisciotto, Allan, et al., 1990; Ingle, Suyehiro, von Breymann, et al., 1990). Petrologic study of the aliquots of the samples is reported elsewhere, including chemical analyses by X-ray fluorescence (Yamashita and Fujii, this volume).

Most of the rocks from Sites 794 and 797 were emplaced as basaltic sills (Tamaki, Pisciotto, Allan, et al., 1990), which made them nearly holocrystalline dolerites and basalts during solidification except for in the marginal parts of the sills. Although they are generally highly altered to form large amounts of clay minerals replacing primary constituent minerals and subordinate mesostasis in thin section, some (in particular, the internal part of a sill) remain their primary mineralogy. In these samples, the constituent minerals are fresh except for olivine. Such samples were used for the present study.

The rocks from Site 795 occur as subaqueous basaltic lava flows (Tamaki, Pisciotto, Allan, et al., 1990). Compared with the rocks from Sites 794 and 797, they commonly contain larger amounts of mesostasis and vesicles, which have been altered to form clay minerals. Although we tried to find the most suitable rock samples for ^{40}Ar-^{39}Ar

[1] Tamaki, K., Suyehiro, K., Allan, J., McWilliams, M., et al., 1992. *Proc. ODP, Sci. Results,* 127/128, Pt. 2: College Station, TX (Ocean Drilling Program).
[2] Earthquake Research Institute, University of Tokyo, Bunkyo-ku, Tokyo 113, Japan.
[3] Kanto Gakuen University, Ohta-shi, Gunma Prefecture 373, Japan.
[4] Department of Earth Sciences, Faculty of Science, Yamagata University, Koshirakawa-cho, Yamagata 990, Japan (Present address: Department of Earth and Planetary Sciences, Faculty of Science, Kyushu University, Higashi-ku, Fukuoka 812, Japan).
[5] Ocean Research Institute, University of Tokyo, Nakeno-ku, Tokyo 164, Japan.

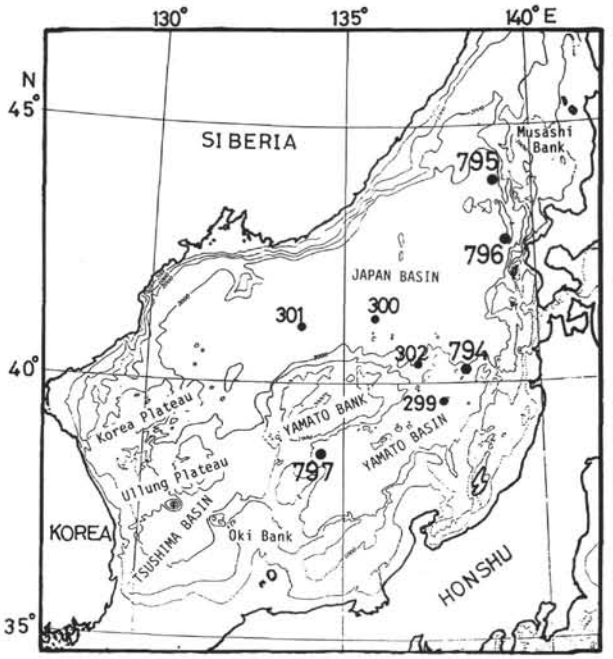

Figure 1. Leg 127 Sites 794–797, Leg 128 Site 794, and Deep Sea Drilling Project Leg 31 Sites 299–302. ^{40}Ar-^{39}Ar analyses were performed for basement volcanic rocks recovered from Sites 797, 794, and 795.

dating, constituent minerals such as plagioclase and clinopyroxene are partially altered in the selected samples. The number of samples selected for the present study reflects this situation.

EXPERIMENTAL METHODS

Rock samples were cut as cylinders (6 mm diameter × 10 mm long) and stacked in quartz ampoules (10 mm diameter × 70 mm long) together with standard biotites (JB-1 biotite; age: 90.8 ± 1.5 Ma, K: 6.34 ± 0.04 wt%), CaF_2, and K_2SO_4. They were irradiated with a fast neutron flux of 1×10^{17} to 5×10^{17} n/cm^2 using the Japan Material Test Reactor of Tohoku University. Because of the limited number of ampoules that could be irradiated at one time, the samples were irradiated in batches, with somewhat different irradiation conditions among the samples. Hence, different correction factors were used to correct for K- and Ca-derived interference Ar isotopes, which were determined for each irradiation session on the basis of Ar analyses of the irradiated CaF_2 and K_2SO_4.

Ar was extracted in increasing temperature steps using an induction furnace and purified according to conventional procedures at the Isotope Center, University of Tokyo. The temperature during each heating step was maintained for 45 to 60 min. The Ar isotopes were analyzed by two methods. Seven samples were analyzed using a quadrupole mass spectrometer installed in the Isotope Center and connected directly to the Ar-extraction and -purification system. The experimental conditions of the quadrupole mass spectrometer have been reported in Takigami et al. (1984). Because the analytical precision of this mass spectrometer is not sufficient to give confident numbers in the present age range, we used another mass spectrometer to analyze the other six samples for comparison of the obtained ages. For these six samples, purified Ar gases from each temperature fraction were stored in glass ampoules and analyzed on a sector-type mass spectrometer at Yamagata University. The experimental conditions of this mass spectrometer have been reported previously (Takaoka, 1976).

Uncertainties in the obtained ^{40}Ar-^{39}Ar ages reflect those of the isotopic ratios and the J value, including the uncertainty derived from the age of the standard, but do not include those derived from the correction factors for K- and Ca-derived interference Ar isotopes.

RESULTS

The results of the ^{40}Ar-^{39}Ar analyses for each sample are given in Table 1 and summarized in Table 2. The ^{40}Ar-^{39}Ar age spectra are shown together with isochron plots in Figures 2A–2L, except for Sample 127-797C-21R-5. A reference isochron is drawn for each isochron plot. Because Sample 127-797C-21R-5 produced a large uncertainty in the age of each temperature fraction, its spectrum is not included here.

Three of the five samples from Site 797 indicate plateau ages of 18–20 Ma, but the other two do not exhibit plateaus. Although Sample 127-797C-21R-5 includes large uncertainties in the ages obtained for each fraction, the total recombined gas age indicates about 20 Ma. In the case of Sample 127-797C-27R-1, the total ^{40}Ar-^{39}Ar age is 20.8 Ma, whereas the ^{40}Ar-^{39}Ar plateau age indicates 19.0 ± 1.1 Ma. The slightly higher value in the total ^{40}Ar-^{39}Ar age would reflect the occurrence of a small amount of excess ^{40}Ar in the highest temperature fraction and may also reflect a partial ^{39}Ar loss in the lowest temperature fraction. Because the plateau range covers more than 80% of the integrated ^{39}Ar, the calculated plateau age probably represents the formation age of the sample. Gases from the 800° and 900°C temperature fractions were lost when the seals broke on the tubes before the analysis of Sample 127-797C-34R-1 and no plateau age could be obtained. However, the 1100°C fraction indicates an ^{40}Ar-^{39}Ar age of about 17 Ma with a relatively large proportion to the remaining total ^{39}Ar. The rate of ^{39}Ar lost from some of the temperature fractions could be roughly estimated by comparing the amount of integrated ^{39}Ar observed with that of the ^{39}Ar calculated from the K content of the sample, which indicates a range of several percent to about 15% for the samples. Hence, 10% was assumed as the rate of ^{39}Ar lost for each temperature fraction concerned. Further, the integrated ^{40}Ar-^{39}Ar age calculated for the remaining fractions is 20 Ma. Hence, the value might not be so different from the formation age for this sample. Sample 127-797C-41R-1 indicates a good plateau age of 19.0 ± 0.3 Ma, covering about two-thirds of the integrated ^{39}Ar. The total age is about 20 Ma. Hence, the plateau age probably reflects the formation age for this sample. On the other hand, Sample 127-797C-45R-2 shows a slightly younger plateau age of 17.7 ± 0.5 Ma for the temperature fractions 800°–1000°C than the age of Sample 127-797C-41R-1. The plateau range for Sample 127-797C-45R-2 covers about 45% of the total ^{39}Ar, which is slightly narrower than those of the other samples.

The samples from Hole 794C were recovered during Leg 127, whereas Hole 794D was drilled during Leg 128 at the same site. Sample 127-794C-3R-1 shows a plateaulike age of 20.6 ± 0.6 Ma. For this sample, the lower temperature fractions show slightly higher values and the higher temperature fractions lower values. Sample 127-794C-8R-1 indicates a plateau age of 20.0 Ma, but it is accompanied by a relatively large uncertainty of ±2.0 Ma. On the other hand, the three samples from Hole 794D show ^{40}Ar-^{39}Ar ages of 20–21 Ma. Sample 128-794D-15R-1 indicates a relatively good plateau age of 19.9 ± 0.7 Ma. The 1100°C fraction was lost from Sample 128-794D-17R-1 and no plateau age was developed. However, the 1000°C fraction indicates a ^{40}Ar-^{39}Ar age of 20.9 ± 0.9 Ma with more than 50% of the integrated ^{39}Ar. Hence, the 1000°C fraction may approximate the formation age of this sample. The 900°C fraction was lost for Sample 128-794D-20R-1, but the 1000°–1200°C fractions form a relatively good plateau age of 21.2 ± 0.8 Ma with a relatively large fraction of the integrated ^{39}Ar. Thus, we found no systematic differences in the ages obtained from the samples from Holes 794C and 794D.

The three samples from Site 795 show rather disturbed patterns, probably reflecting the greater extent of alteration of the samples.

Plateaulike ages range from 17 to 24 Ma for the Site 795 samples, but the fractions of ^{39}Ar represented by these steps are relatively small (less than 36%). Further, the three samples show total ages of more than 30 Ma, systematically higher than those from Sites 797 and 794 in the Yamato Basin. The occurrence of excess ^{40}Ar together with partial ^{39}Ar loss might be possible in these samples.

DISCUSSION

Comparison of ^{40}Ar-^{39}Ar Ages Determined Under Different Analytical Conditions

As mentioned previously, the samples were analyzed under different experimental conditions, including different neutron irradiation and analytical facilities. Within this set of ^{40}Ar-^{39}Ar ages, however, no systematic differences can be distinguished. For example, in the case of samples from Site 794, the Hole 794C samples were analyzed on the quadrupole mass spectrometer with an on-line extraction and purification system, whereas the samples from Hole 794D were analyzed on the sector-type mass spectrometer with a system separated from an extraction and purification line. As shown in Table 2 and Figure 3, the results from the two holes and systems agree with one another within the experimental uncertainties. In the preliminary analyses, the values obtained by the quadrupole mass spectrometer were slightly younger than the present ones by 1–2 Ma. However, the correction for the tailing effect had not been well evaluated when the Ca-interference Ar isotopes were examined and the value $(^{36}Ar/^{37}Ar)_{Ca}$ increased after the correction, resulting in an increase in the calculated ages by 1–2 Ma.

Two of the samples from Site 797 show ^{40}Ar-^{39}Ar plateau ages of about 19 Ma, whereas the other two have ages of 17–18 Ma. No systematic differences were observed between the analyses using different mass spectrometers under different conditions. Thus, the good agreement in the ages obtained under different analytical conditions would argue that most of the systematic errors are insignificant and support the reliability of the calculated values.

Precision in the calculated ages is generally better for the ages obtained by the sector-type mass spectrometer than that obtained by the quadrupole mass spectrometer. The precision is reflected in the uncertainty of calculated ages.

Evaluation of the ^{40}Ar-^{39}Ar Ages Obtained

It is well known that K-Ar systematics for submarine rocks are liable to be affected by alteration with seawater and the occurrence of excess ^{40}Ar. To minimize such possibilities, the precautions of selecting rock samples that are as fresh as possible and excluding glassy samples and those containing giant phenocrysts were followed carefully in this study.

In all of the samples we found minor amounts of glassy parts (less than several percent), but the mesostasis in the samples from Hole 795B was found to be more abundant than that in samples from the other holes. Mesostasis in the samples is altered, but the degree of alteration in the phenocrysts varies widely among the samples. Most K is regarded as retained in plagioclase and glass. Because the glass content is not large in the samples, however, the behavior of ^{39}Ar produced from ^{39}K by neutron irradiation would be controlled largely by the distribution and state of the plagioclase in the phenocrysts and mesostasis.

On the other hand, if some excess ^{40}Ar had remained, olivine and clinopyroxene become possible hosts to retain it. The age spectra for samples from Hole 795B surely reflect such combined effects. Hence, their total ages together with their pseudo-plateau ages with narrow ^{39}Ar ranges of 20%–30% should be considered as giving only a rough estimate for the possible ranges of their crystallization ages.

In the age spectra, apparently high ^{40}Ar-^{39}Ar ages in the lower temperature fractions for the samples might reflect either selective ^{39}Ar loss from a sample due to a recoil effect of ^{39}Ar or redistribution of radiogenic ^{39}Ar trapped at a relatively loose site during neutron irradiation. On the other hand, the apparently high ^{40}Ar-^{39}Ar ages observed in the higher or highest temperature fractions possibly indicate the occurrence of excess ^{40}Ar. Such phenomena were found for samples from Holes 794C, 794D, and 797C. For example, Sample 128-794D-15R-1 is a typical case with a relatively good plateau age in the intermediate temperature fractions (Fig. 2G). In this study, a plateau age is defined by ages that overlap each other within their analytical uncertainties through more than three successive temperature fractions and the integrated ^{39}Ar covers more than 40% of the total ^{39}Ar observed. The limit for the amount of integrated ^{39}Ar as a plateau range is not definitive.

Among the seven samples that appear to show plateau ages, however, Sample 127-794C-3R-1 (plagioclase-pyroxene phyric leucocratic dolerite) has a typical reversed stairstep pattern. Although there is no feasible reason why this rock would be affected by neutron irradiation petrographically, the pattern of the age spectrum suggests the possibility of the total redistribution of Ar in this sample. If this was the case, the total age would be closer to the crystallization age. In effect, the total age and the apparent plateau age for this sample are similar and the age of about 21 Ma is probably not much different from the crystallization age. However, we distinguish this value from a typical plateau age by putting it in parentheses in Table 2.

In the case of Sample 127-797C-45R-2, the plateau range covers only about 44% of the integrated ^{39}Ar of the total ^{39}Ar (Fig. 2D). However, three successive temperature fractions (800°–1000°C) indicate similar ages with 17.7 ± 0.5 Ma as an average. We do not think that this is an artifact and regard it as meaningful geologically.

Sample 127-794C-8R-1 indicates a plateau age of 20.0 Ma, but it is accompanied by relatively large analytical uncertainties for each temperature fraction (Fig. 2F). Such large analytical uncertainties are reflected in the calculated age for this sample (cf. Table 2). Although the plateau age for this sample includes a relatively large uncertainty, we have no reason to discard it as meaningless.

The other four samples—127-797C-27R-1 (Fig. 2A), 127-797C-41R-1 (Fig. 2C), 128-794D-15R-1 (Fig. 2G), and 128-794D-20R-1 (Fig. 2I)—show relatively good plateau ages in the intermediate temperature fractions with coverage of more than 65% of the integrated ^{39}Ar. Thus, the results from these samples give strong constraints concerning the formation age of the ocean floor in the Japan Sea.

Comparison with Ages Estimated by Paleontology

The results from this study are plotted in Figure 3 for the lithofacies encountered at the Leg 127 sites (Tamaki, Pisciotto, Allan, et al., 1990). The results for the samples recovered at Site 794 during Leg 128 are also shown by extending the stratigraphic column to indicate the relative recovered depths.

Although volcanic rocks were recovered from the Japan Sea floor during Legs 127 and 128, the acoustic basement is composed of interlayered basalts (sills and flows) and sediments (Tamaki, Pisciotto, Allan, et al., 1990). Thus, uncertainty remains about whether drilling reached the bottom of the basin sediments. The samples recovered, however, may at least give some age constraints on the age of basin formation based on micropaleontological data, such as rare occurrences of calcareous nannofossils and planktonic foraminifers in the sediments and diatoms in dolomite nodules. According to such paleontological constraints, the ages of the shallow sediment/basalt contacts have been estimated as follows: Site 797, 19 Ma; Site 794, 15.5 Ma; Site 795, 14 Ma (Tamaki, Pisciotto, Allan, et al., 1990).

Table 1. Ar isotopes in neutron-irradiated rocks recovered from the Japan Sea floor.

127-797C-21R-5 (Aphyric dolerite, 1.828 g, J = 0.003536± 0.000070, correction factor = a, mass spectrometer = QMS)

Temperature (°C)	$^{40}Ar^{a}$ ($\times 10^{-9}$ cm^3 STP/g)	$^{39}Ar^{*}$ (%)	$^{36}Ar/^{40}Ar$ ($\times 10^{-3}$)	$^{37}Ar/^{40}Ar$ ($\times 10^{-1}$)	$^{39}Ar/^{40}Ar$ ($\times 10^{-2}$)	$^{40}Ar^{*}/^{39}Ar^{*b}$	Age^{c} (Ma)
<600	2.79	0.2	5.211 ±0.658	0.5030 ±0.0616	1.491 ±0.184	−41.06 ±17.27	−245 ±103
600	53.9	1.4	3.776 ±0.087	0.8512 ±0.0106	0.6205 ±0.0072	−17.55 ±5.75	−109 ±36
700	36.8	1.1	3.681 ±0.072	0.7442 ±0.0089	0.7572 ±0.0174	−10.34 ±3.79	−64.8 ±23.8
800	34.7	1.8	3.675 ±0.136	1.801 ±0.020	1.249 ±0.014	−4.422 ±4.465	−28.0 ±28.3
900	70.0	7.3	3.690 ±0.080	3.609 ±0.040	2.564 ±0.017	−1.958 ±2.980	−12.5 ±19.0
1000	218	24.0	3.322 ±0.051	3.044 ±0.033	2.705 ±0.017	2.774 ±1.404	17.6 ±8.9
1100	54.0	24.3	3.563 ±0.263	18.54 ±0.18	11.10 ±0.12	2.659 ±1.969	16.9 ±12.5
1200	27.8	15.2	3.819 ±0.181	29.31 ±0.33	13.63 ±0.11	3.138 ±2.036	19.9 ±12.9
1300	12.8	11.3	7.501 ±0.469	94.27 ±0.78	22.84 ±0.23	1.853 ±3.198	11.8 ±20.3
1500	55.4	13.4	8.012 ±0.227	92.03 ±0.77	7.319 ±0.039	5.524 ±12.034	34.9 ±76.0
Total	566.19	100.0	4.066	16.20	4.511	3.210	20.4

127-797C-27R-1 (Aphyric basalt, 1.366 g, J = 0.003869±0.000078, correction factor = a, mass spectrometer = QMS)

Temperature (°C)	$^{40}Ar^{a}$ ($\times 10^{-9}$ cm^3 STP/g)	$^{39}Ar^{*}$ (%)	$^{36}Ar/^{40}Ar$ ($\times 10^{-3}$)	$^{37}Ar/^{40}Ar$ ($\times 10^{-1}$)	$^{39}Ar/^{40}Ar$ ($\times 10^{-1}$)	$^{40}Ar^{*}/^{39}Ar^{*b}$	Age^{c} (Ma)
<600	3.32	0.1	n.d.	0.2639 ±0.0081	±0.2168 ±0.0064	±25.34 ±20.70	±169 ±138
600	28.8	1.7	2.855 ±0.153	1.405 ±0.016	0.5643 ±0.0060	3.177 ±0.983	22.0 ±6.8
700	37.4	9.4	1.511 ±0.064	4.767 ±0.059	2.316 ±0.022	2.671 ±0.242	18.9 ±1.8
800	39.0	11.2	1.129 ±0.058	5.371 ±0.063	2.633 ±0.015	2.852 ±0.230	19.8 ±1.7
900	60.6	23.6	0.7701 ±0.0637	12.88 ±0.16	3.597 ±0.021	2.605 ±0.171	18.1 ±1.2
1000	87.0	27.4	1.452 ±0.033	13.42 ±0.15	2.909 ±0.017	2.784 ±0.403	19.3 ±2.8
1100	33.6	12.5	±0.9077 ±0.0453	17.39 ±0.19	3.437 ±0.020	2.757 ±0.158	19.1 ±1.2
1200	22.6	6.3	1.003 ±0.044	13.54 ±0.16	2.592 ±0.018	3.544 ±0.354	24.6 ±2.5
1300	14.6	3.6	2.579 ±0.085	18.14 ±0.16	2.265 ±0.025	2.521 ±0.717	17.5 ±5.0
1500	92.0	4.2	3.685 ±0.109	20.74 ±0.23	0.4491 ±0.0031	5.861 ±2.598	40.50 ±18.0
Total	418.92	100.0	1.875	12.99	2.210	2.991	20.8

The present results agree well with the biostratigraphic age estimate at Site 797, but indicate older ages at Sites 794 and 795. As discussed previously, the ^{40}Ar-^{39}Ar ages obtained for samples at Site 794 were analyzed at different facilities under different experimental conditions and show similar ages of about 20 Ma. Further, most of them indicate reasonable ^{40}Ar-^{39}Ar plateau ages and no significant increase in the $^{40}Ar/^{36}Ar$ intercept is expected in the isochron plots (Fig. 2). They imply no occurrence of significant amounts of excess ^{40}Ar in these samples. Hence, it appears that the ^{40}Ar-^{39}Ar plateau ages are reliable crystallization ages and that an age gap exists.

The samples from Site 795 show rather poor plateaulike ages. If we accept their lower values, the samples from Site 795 indicate ^{40}Ar-^{39}Ar ages of about 13–17 Ma, which does not seem incompatible with the ages estimated from paleontological data.

Table 1 (continued).

127-797C-34R-1 (Aphyric basalt, 1.631 g, J = 0.003430± 0.000057, correction factor = b, mass spectrometer = sector type)

Temperature (°C)	^{40}Ar[a] ($\times 10^{-9}$ cm^3 STP/g)	^{39}Ar* (%)	^{36}Ar/^{40}Ar ($\times 10^{-3}$)	^{37}Ar/^{40}Ar ($\times 10^{-1}$)	^{39}Ar/^{40}Ar ($\times 10^{-1}$)	^{40}Ar*/^{39}Ar*[b]	Age[c] (Ma)
600	15.7	0.1	3.266 ±0.043	0.09604 ±0.00110	0.02729 ±0.00012	13.99 ±4.70	84.5 ±27.8
700	58.6	1.8	1.503 ±0.032	0.5224 ±0.0038	0.3007 ±0.0027	19.08 ±0.36	114 ±3
800	–	[d]10.0	–	–	–	–	–
900	–	[d]10.0	–	–	–	–	–
1000	255	5.9	3.161 ±0.051	0.3905 ±0.0013	0.2204 ±0.0016	3.529 ±0.687	21.7 ±4.2
1100	171	41.0	1.444 ±0.023	2.298 ±0.027	2.289 ±0.007	2.810 ±0.031	17.3 ±0.3
1200	128	15.5	2.678 ±0.079	1.140 ±0.022	1.162 ±0.011	2.093 ±0.202	12.9 ±1.3
1600	137	15.7	3.957 ±0.080	18.42 ±0.33	1.144 ±0.017	3.447 ±0.221	21.2 ±1.4
Total	765.3	100.0	2.713	4.201	0.9980	3.230	19.9

127-797C-41R-1 (Sparsely plagioclase phyric basalt, 1.436 g, J = 0.003500±0.000058, correction factor = b, mass spectrometer = sector type)

Temperature (°C)	^{40}Ar[a] ($\times 10^{-9}$ cm^3 STP/g)	^{39}Ar* (%)	^{36}Ar/^{40}Ar ($\times 10^{-3}$)	^{37}Ar/^{40}Ar ($\times 10^{-1}$)	^{39}Ar/^{40}Ar ($\times 10^{-1}$)	^{40}Ar*/^{39}Ar*[b]	Age[c] (Ma)
600	19.5	0.1	3.098 ±0.047	0.1447 ±0.0071	0.04010 ±0.00033	22.33 ±3.50	136 ±21
700	81.4	0.5	3.250 ±0.024	0.1156 ±0.0020	0.04824 ±0.00019	8.993 ±1.478	55.5 ±9.1
800	21.4	1.6	2.788 ±0.039	0.7692 ±0.0018	0.5496 ±0.0018	3.603 ±0.211	22.6 ±1.4
900	50.7	8.1	2.103 ±0.032	1.755 ±0.012	1.201 ±0.006	3.528 ±0.079	22.1 ±0.6
1000	141	26.0	2.276 ±0.014	3.263 ±0.007	1.393 ±0.002	2.996 ±0.030	18.8 ±0.4
1100	135	29.9	2.037 ±0.013	4.353 ±0.009	1.677 ±0.003	3.081 ±0.023	19.4 ±0.4
1200	47.4	12.9	1.692 ±0.027	3.877 ±0.026	2.139 ±0.007	2.913 ±0.076	18.4 ±0.6
1600	322	20.9	3.261 ±0.030	4.684 ±0.023	0.4977 ±0.0013	3.584 ±0.181	22.5 ±1.2
Total	818.4	100.0	2.710	3.492	0.9173	3.238	20.3

127-797C-45R-2 (Aphyric dolerite, 1.665 g, J = 0.003572± 0.000060, correction factor = b, mass spectrometer = sector type)

Temperature (°C)	^{40}Ar[a] ($\times 10^{-9}$ cm^3 STP/g)	^{39}Ar* (%)	^{36}Ar/^{40}Ar ($\times 10^{-3}$)	^{37}Ar/^{40}Ar ($\times 10^{-1}$)	^{39}Ar/^{40}Ar ($\times 10^{-1}$)	^{40}Ar*/^{39}Ar*[b]	Age[c] (Ma)
600	9.2	0.005	3.380 ±0.175	0.06648 ±0.00202	0.005432 ±0.000062	6.773 ±0.360	43.1 ±2.4
700	160	0.8	3.385 ±0.068	0.07618 ±0.00072	0.04787 ±0.00009	0.3398 ±0.0069	2.19 ±0.06
800	56.8	3.2	2.869 ±0.088	0.4910 ±0.0043	0.5697 ±0.0041	2.811 ±0.090	18.0 ±0.7
900	95.8	12.7	2.205 ±0.023	0.7909 ±0.0019	1.325 ±0.003	2.675 ±0.030	17.2 ±0.3

Table 1 (continued).

Temperature (°C)	$^{40}Ar^{a}$ ($\times 10^{-9}$ cm^3 STP/g)	$^{39}Ar^{*}$ (%)	$^{36}Ar/^{40}Ar$ ($\times 10^{-3}$)	$^{37}Ar/^{40}Ar$ ($\times 10^{-1}$)	$^{39}Ar/^{40}Ar$ ($\times 10^{-1}$)	$^{40}Ar^{*}/^{39}Ar^{*b}$	Age^{c} (Ma)
1000	153	28.9	1.956 ±0.017	3.948 ±0.008	1.900 ±0.003	2.781 ±0.032	17.8 ±0.4
1100	98.3	25.5	0.6801 ±0.0106	2.959 ±0.021	2.609 ±0.013	3.297 ±0.104	21.1 ±0.8
1200	75.3	18.8	1.406 ±0.026	2.082 ±0.006	2.501 ±0.005	2.464 ±0.055	15.8 ±0.4
1600	90.0	10.1	3.644 ±0.089	14.80 ±0.07	1.162 ±0.006	3.630 ±0.168	23.2 ±1.1
Total	738.4	100.005	2.366	3.386	1.356	2.908	18.6

127-794C-3R-1 (Plagioclase-pyroxene phyric leucocratic dolerite, 1.354 g, J = 0.003894±0.000078, correction factor = c, mass spectrometer = QMS)

Temperature (°C)	$^{40}Ar^{a}$ ($\times 10^{-9}$ cm^3 STP/g)	$^{39}Ar^{*}$ (%)	$^{36}Ar/^{40}Ar$ ($\times 10^{-3}$)	$^{37}Ar/^{40}Ar$	$^{39}Ar/^{40}Ar$ ($\times 10^{-1}$)	$^{40}Ar^{*}/^{39}Ar^{*b}$	Age^{c} (Ma)
<600	19.6	0.9	3.306 ±0.156	0.2084 ±0.0012	0.5502 ±0.0091	1.124 ±0.844	7.88 ±5.90
600	45.3	4.3	2.605 ±0.163	0.7357 ±0.0108	1.163 ±0.013	3.220 ±0.419	22.5 ±2.9
700	35.5	8.4	0.9896 ±0.0852	1.426 ±0.024	2.882 ±0.023	3.410 ±0.094	23.8 ±0.8
800	74.6	15.0	1.666 ±0.131	1.338 ±0.018	2.464 ±0.020	3.114 ±0.161	21.7 ±1.2
900	80.9	19.1	1.932 ±0.041	1.963 ±0.026	2.890 ±0.020	2.820 ±0.050	19.7 ±0.5
1000	61.6	16.5	1.498 ±0.049	2.090 ±0.026	3.280 ±0.021	2.947 ±0.051	20.6 ±0.5
1100	48.3	14.7	0.6498 ±0.0375	0.8920 ±0.0110	3.696 ±0.024	2.610 ±0.035	18.2 ±0.4
1200	46.8	14.8	0.7341 ±0.0374	0.7609 ±0.0104	3.845 ±0.023	2.369 ±0.033	16.6 ±0.4
1300	14.6	3.6	1.568 ±0.095	1.909 ±0.031	2.994 ±0.025	3.042 ±0.101	21.3 ±0.8
1500	25.8	2.7	5.533 ±0.097	8.207 ±0.097	1.382 ±0.014	8.046 ±0.284	55.7 ±2.2
Total	453.0	100.0	1.815	1.753	2.700	2.990	20.9

127-794C-8R-1 (Aphyric dolerite, 1.297 g, J = 0.003946±0.000079, correction factor = c, mass spectrometer = QMS)

Temperature (°C)	$^{40}Ar^{a}$ ($\times 10^{-9}$ cm^3 STP/g)	$^{39}Ar^{*}$ (%)	$^{36}Ar/^{40}Ar$ ($\times 10^{-3}$)	$^{37}Ar/^{40}Ar$ ($\times 10^{-2}$)	$^{39}Ar/^{40}Ar$ ($\times 10^{-2}$)	$^{40}Ar^{*}/^{39}Ar^{*b}$	Age^{c} (Ma)
<600	606	1.3	3.355 ±0.048	0.4742 ±0.0186	0.3216 ±0.0023	2.895 ±4.405	20.5 ±31.0
600	1870	14.3	3.277 ±0.038	0.9954 ±0.0168	1.116 ±0.004	2.942 ±1.016	20.8 ±7.2
700	816	23.9	2.989 ±0.033	4.430 ±0.057	4.269 ±0.020	2.870 ±0.233	20.3 ±1.7
800	649	22.6	2.975 ±0.048	9.332 ±0.098	5.065 ±0.034	2.693 ±0.280	19.1 ±2.0
900	386	11.1	3.002 ±0.046	23.00 ±0.26	4.203 ±0.022	3.751 ±0.328	26.5 ±2.4
1000	315	9.7	3.062 ±0.046	45.31 ±0.59	4.516 ±0.025	4.135 ±0.309	29.2 ±2.2

Table 1 (continued).

Temperature (°C)	$^{40}Ar^a$ ($\times 10^{-9}$ cm^3 STP/g)	$^{39}Ar^*$ (%)	$^{36}Ar/^{40}Ar$ ($\times 10^{-3}$)	$^{37}Ar/^{40}Ar$ ($\times 10^{-2}$)	$^{39}Ar/^{40}Ar$ ($\times 10^{-2}$)	$^{40}Ar^*/^{39}Ar^{*b}$	Age^c (Ma)
1100	46.8	7.8	1.974 ±0.045	129.8 ±1.8	24.37 ±0.16	2.739 ±0.060	19.4 ±0.6
1200	27.4	5.5	1.809 ±0.096	92.30 ±1.50	29.35 ±0.24	2.159 ±0.099	15.3 ±0.8
1300	13.0	2.7	2.444 ±0.096	230.2 ±3.5	30.68 ±0.22	2.384 ±0.098	16.9 ±0.8
1500	17.3	1.1	5.096 ±0.121	629.5 ±7.5	9.825 ±0.063	8.528 ±0.432	59.7 ±3.2
Total	4746.5	100.0	3.142	12.12	3.081	3.059	21.7

128-794D-15R-1 (Aphyric dolerite, 1.270 g, J = 0.003185±0.000100, correction factor = b, mass spectrometer = sector type)

Temperature (°C)	$^{40}Ar^a$ ($\times 10^{-9}$ cm^3 STP/g)	$^{39}Ar^*$ (%)	$^{36}Ar/^{40}Ar$ ($\times 10^{-3}$)	$^{37}Ar/^{40}Ar$ ($\times 10^{-1}$)	$^{39}Ar/^{40}Ar$ ($\times 10^{-1}$)	$^{40}Ar^*/^{39}Ar^{*b}$	Age^c (Ma)
600	7.1	0.1	3.104 ±0.261	0.3307 ±0.0054	0.03018 ±0.00032	13.67 ±26.22	76.9 ±144.4
700	93.1	2.7	3.308 ±0.020	0.8383 ±0.0024	0.05270 ±0.00033	6.470 ±1.166	36.8 ±6.7
800	58.5	4.8	3.136 ±0.034	2.819 ±0.007	0.1519 ±0.0005	7.403 ±0.692	42.0 ±4.1
900	68.4	25.7	3.197 ±0.034	14.76 ±0.07	0.6946 ±0.0021	3.568 ±0.153	20.4 ±1.1
1000	76.3	35.9	3.321 ±0.030	22.15 ±0.07	0.8780 ±0.0028	3.497 ±0.108	20.0 ±0.9
1100	14.7	11.1	3.664 ±0.070	41.81 ±0.15	1.422 ±0.008	3.231 ±0.157	18.5 ±1.1
1200	8.9	3.3	3.459 ±0.060	20.50 ±0.15	0.6809 ±0.0042	3.605 ±0.281	20.6 ±1.7
1600	35.6	16.4	7.183 ±0.017	132.4 ±0.4	1.115 ±0.003	6.132 ±0.066	34.9 ±1.2
Total	362.6	100.0	3.657	23.34	0.4838	4.202	24.0

128-794D-17R-1 (Aphyric basalt, 1.079 g, J = 0.003485±0.000100, corrector factor = b, mass spectrometer = sector type)

Temperature (°C)	$^{40}Ar^a$ ($\times 10^{-9}$ cm^3 STP/g)	$^{39}Ar^*$ (%)	$^{36}Ar/^{40}Ar$ ($\times 10^{-3}$)	$^{37}Ar/^{40}Ar$ ($\times 10^{-1}$)	$^{39}Ar/^{40}Ar$ ($\times 10^{-2}$)	$^{40}Ar^*/^{39}Ar^{*b}$	Age^c (Ma)
600	75.8	0.4	3.007 ±0.034	0.05097 ±0.00143	0.1324 ±0.0037	85.36 ±8.03	470 ±41
700	112	1.5	3.222 ±0.011	0.4696 ±0.0009	0.3589 ±0.0025	15.37 ±0.94	94.1 ±6.2
800	101	2.0	3.302 ±0.025	0.5233 ±0.0034	0.5189 ±0.0057	6.066 ±1.458	37.7 ±9.0
900	125	10.2	3.138 ±0.026	1.550 ±0.006	2.103 ±0.008	4.419 ±0.371	27.6 ±2.4
1000	316	53.9	3.125 ±0.017	5.676 ±0.018	4.463 ±0.013	3.348 ±0.116	20.9 ±0.9
1100	–	[d]10.0	–	–	–	–	–
1200	124	10.2	3.176 ±0.022	2.772 ±0.010	2.163 ±0.010	4.535 ±0.311	28.3 ±2.1
1600	434	11.8	3.527 ±0.015	8.601 ±0.024	0.8844 ±0.0035	10.24 ±0.65	63.3 ±4.3
Total	1287.8	100.0	3.282	4.794	1.772	5.125	31.9

Table 1 (continued).

128-794D-20R-1 (Aphyric dolerite, 1.565 g, J = 0.003485±0.000100, corrector factor = b, mass spectrometer = sector type)

Temperature (°C)	$^{40}Ar^{a}$ ($\times 10^{-9}$ cm^3 STP/g)	$^{39}Ar^{*}$ (%)	$^{36}Ar/^{40}Ar$ ($\times 10^{-3}$)	$^{37}Ar/^{40}Ar$ ($\times 10^{-1}$)	$^{39}Ar/^{40}Ar$ ($\times 10^{-1}$)	$^{40}Ar^{*}/^{39}Ar^{*b}$	Age^{c} (Ma)
600	14.9	3.8	3.254 ±0.117	7.609 ±0.036	0.07457 ±0.00114	23.08 ±6.10	140 ±36
700	129	1.8	3.290 ±0.020	0.2147 ±0.0006	0.03068 ±0.00039	10.09 ±1.96	62.4 ±12.0
800	190	1.3	3.297 ±0.018	0.1878 ±0.0008	0.01488 ±0.00026	19.45 ±3.70	118 ±22
900	–	[d]10.0	–	–	–	–	–
1000	286	41.2	3.301 ±0.011	6.714 ±0.030	0.3332 ±0.0007	3.334 ±0.102	20.8 ±0.9
1100	46.1	24.2	2.742 ±0.064	17.46 ±0.09	1.200 ±0.003	3.410 ±0.160	21.3 ±1.2
1200	20.4	7.3	3.143 ±0.088	18.13 ±0.06	0.8360 ±0.0068	3.640 ±0.325	22.7 ±2.1
1600	79.0	10.4	5.238 ±0.038	61.51 ±0.12	0.4346 ±0.0017	6.956 ±0.386	43.2 ±2.2
Total	765.4	100.0	3.441	8.502	0.2103	4.998	31.2

127-795B-36R-2 (Silicified plagioclase phyric basalt, 1.105 g, J = 0.003196±0.000065, corrector factor = d, mass spectrometer = QMS)

Temperature (°C)	$^{40}Ar^{a}$ ($\times 10^{-9}$ cm^3 STP/g)	$^{39}Ar^{*}$ (%)	$^{36}Ar/^{40}Ar$ ($\times 10^{-3}$)	$^{37}Ar/^{40}Ar$ ($\times 10^{-1}$)	$^{39}Ar/^{40}Ar$ ($\times 10^{-1}$)	$^{40}Ar^{*}/^{39}Ar^{*b}$	Age^{c} (Ma)
<600	54.4	8.4	1.878 ±0.046	0.5634 ±0.0130	0.9918 ±0.0057	4.506 ±0.141	25.8 ±1.0
600	102	19.2	1.646 ±0.040	1.176 ±0.017	1.202 ±0.007	4.370 ±0.102	25.0 ±0.8
700	51.0	13.3	1.675 ±0.040	5.050 ±0.062	1.669 ±0.015	3.518 ±0.078	20.2 ±0.6
800	13.7	6.8	2.206 ±0.168	20.46 ±0.25	3.168 ±0.021	2.244 ±0.159	12.9 ±1.0
900	18.4	6.9	2.774 ±0.133	27.40 ±0.33	2.417 ±0.019	2.833 ±0.168	16.3 ±1.0
1000	15.9	5.9	3.558 ±0.114	40.48 ±0.50	2.399 ±0.017	2.940 ±0.151	16.9 ±0.9
1100	16.2	7.4	2.437 ±0.134	35.11 ±0.43	2.956 ±0.023	3.142 ±0.141	18.0 ±0.9
1200	24.3	13.3	2.233 ±0.112	24.36 ±0.29	3.509 ±0.020	2.207 ±0.097	12.7 ±0.6
1300	23.9	12.0	2.009 ±0.122	20.17 ±0.26	3.223 ±0.020	2.368 ±0.115	13.6 ±0.7
1500	60.1	6.8	4.972 ±0.112	38.28 ±0.42	0.7739 ±0.0040	6.940 ±0.470	39.6 ±2.8
Total	379.9	100.0	2.320	15.23	1.697	3.493	20.0

127-795B-38R-4 (Sparsely pyroxene-plagioclase phyric basalt, 1.154 g, J = 0.003275±0.000066, correction factor = d, mass spectrometer = QMS)

Temperature (°C)	$^{40}Ar^{a}$ ($\times 10^{-9}$ cm^3 STP/g)	$^{39}Ar^{*}$ (%)	$^{36}Ar/^{40}Ar$ ($\times 10^{-3}$)	$^{37}Ar/^{40}Ar$	$^{39}Ar/^{40}Ar$ ($\times 10^{-1}$)	$^{40}Ar^{*}/^{39}Ar^{*b}$	Age^{c} (Ma)
<600	17.5	3.0	2.711 ±0.117	0.1689 ±0.0026	0.5428 ±0.0051	4.177 ±0.641	24.5 ±3.8
600	24.2	8.6	1.585 ±0.036	0.4367 ±0.0061	1.142 ±0.006	5.308 ±0.098	31.1 ±0.9

Table 1 (continued).

Temperature (°C)	^{40}Ar[a] ($\times 10^{-9}$ cm^3 STP/g)	^{39}Ar* (%)	^{36}Ar/^{40}Ar ($\times 10^{-3}$)	^{37}Ar/^{40}Ar	^{39}Ar/^{40}Ar ($\times 10^{-1}$)	^{40}Ar*/^{39}Ar*[b]	Age[c] (Ma)
700	27.4	10.8	2.710 ±0.086	0.6086 ±0.0074	1.262 ±0.010	2.410 ±0.203	14.2 ±1.2
800	24.4	13.1	2.754 0.104	1.518 ±0.017	1.736 ±0.009	2.660 ±0.180	15.7 ±1.1
900	14.9	9.0	3.195 ±0.196	3.295 ±0.038	1.974 ±0.015	3.410 ±0.303	20.0 ±1.8
1000	36.6	10.6	3.620 ±0.116	2.150 ±0.027	0.9529 ±0.0087	3.531 ±0.375	20.7 ±2.2
1100	16.7	15.8	3.195 ±0.120	5.250 ±0.066	3.092 ±0.022	3.211 ±0.023	18.9 ±0.4
1200	20.7	14.2	2.754 ±0.116	1.960 ±0.025	2.219 ±0.018	2.440 ±0.158	14.4 ±1.0
1300	27.1	10.0	3.440 ±0.078	2.470 ±0.023	1.206 ±0.013	3.729 ±0.205	21.9 ±1.3
1500	121	4.9	3.778 ±0.065	1.799 ±0.020	0.1502 ±0.0015	17.29 ±1.55	99.4 ±8.9
Total	330.5	100.0	3.232	1.839	0.9890	3.940	23.1

127-795B-41R-1 (Sparsely pyroxene-plagioclase phyric basalt, 1.274 g, J = 0.003369±0.000068, correction factor = d, mass spectrometer = QMS)

Temperature (°C)	^{40}Ar[a] ($\times 10^{-9}$ cm^3 STP/g)	^{39}Ar* (%)	^{36}Ar/^{40}Ar ($\times 10^{-3}$)	^{37}Ar/^{40}Ar	^{39}Ar/^{40}Ar ($\times 10^{-2}$)	^{40}Ar*/^{39}Ar*[b]	Age[c] (Ma)
<600	47.6	14.8	2.327 ±0.057	0.1722 ±0.0027	8.427 ±0.054	4.010 ±0.203	24.2 ±1.3
600	54.0	15.4	2.509 ±0.052	0.2349 ±0.0029	7.743 ±0.075	3.835 ±0.204	23.2 ±1.3
700	38.6	11.0	2.883 ±0.074	0.4167 ±0.0054	7.819 ±0.079	2.827 ±0.282	17.1 ±1.7
800	35.8	15.6	2.558 ±0.087	1.257 ±0.015	11.94 ±0.09	3.989 ±0.222	24.1 ±1.4
900	10.3	8.7	3.525 ±0.150	4.553 ±0.053	23.47 ±0.20	3.475 ±0.201	21.0 ±1.3
1000	31.4	6.8	3.309 ±0.098	1.803 ±0.021	6.124 ±0.005	6.043 ±0.497	36.4 ±3.1
1100	10.3	6.6	5.017 ±0.250	6.295 ±0.094	18.20 ±0.15	3.951 ±0.438	23.9 ±2.7
1200	8.31	5.0	3.381 ±0.232	5.146 ±0.073	17.06 ±0.13	5.823 ±0.427	35.1 ±2.6
1300	27.2	6.2	3.808 ±0.092	2.054 ±0.025	6.436 ±0.049	4.148 ±0.447	25.0 ±2.7
1500	141	9.9	3.480 ±0.057	1.528 ±0.017	2.075 ±0.024	13.65 ±0.93	81.1 ±5.4
Total	404.51	100.0	3.124	1.395	6.337	4.990	30.1

Note: All tabulated data corrected for the mass-discrimination effect, the radioactive decay of ^{37}Ar during the period between neutron irradiation and sample analysis, but do not include other corrections. Uncertainties in the measured ratios represent those of the mass spectrometric analyses as 1σ. Correction factor used to estimate ^{40}Ar*/^{39}Ar* depends on the irradiation session:

a $(^{40}Ar/^{39}Ar)_K = 7.31 \times 10^{-2}$ $(^{39}Ar/^{37}Ar)_{Ca} = 1.62 \times 10^{-3}$ $(^{36}Ar/^{37}Ar)_{Ca} = 6.35 \times 10^{-4}$
b $(^{40}Ar/^{39}Ar)_K = 1.62 \times 10^{-1}$ $(^{39}Ar/^{37}Ar)_{Ca} = 2.34 \times 10^{-3}$ $(^{36}Ar/^{37}Ar)_{Ca} = 4.13 \times 10^{-4}$
c $(^{40}Ar/^{39}Ar)_K = 7.80 \times 10^{-2}$ $(^{39}Ar/^{37}Ar)_{Ca} = 1.17 \times 10^{-3}$ $(^{36}Ar/^{37}Ar)_{Ca} = 6.92 \times 10^{-4}$
d $(^{40}Ar/^{39}Ar)_K = 9.20 \times 10^{-2}$ $(^{39}Ar/^{37}Ar)_{Ca} = 1.22 \times 10^{-3}$ $(^{36}Ar/^{37}Ar)_{Ca} = 6.38 \times 10^{-4}$

QMS = quadrupole type.

[a] Amount calculated by assuming the sensitivity of the mass spectrometer, including about 10% uncertainty.

[b] Ratio of radiogenic ^{40}Ar (^{40}Ar*) to K-derived ^{39}Ar (^{39}Ar*) by neutron irradiation.

[c] ^{40}Ar-^{39}Ar age calculated on the basis of the standard JG-1 (biotite): K-Ar age = 90.8 ±1.5 Ma; K = 6.34% ± 0.04%.

[d] Ar gases in the temperature fractions without any indication of the amount of ^{40}Ar and Ar isotopic ratios could not be analyzed when they were lost following breakage of the glass ampoules in which the extracted Ar gases were stored. Based on rough estimates of the rate of ^{39}Ar loss from each temperature fraction from comparison of the amount of integrated ^{39}Ar observed with that of ^{39}Ar calculated from the K content, the degassing rate of ^{39}Ar* in those fractions was assumed to be 10%.

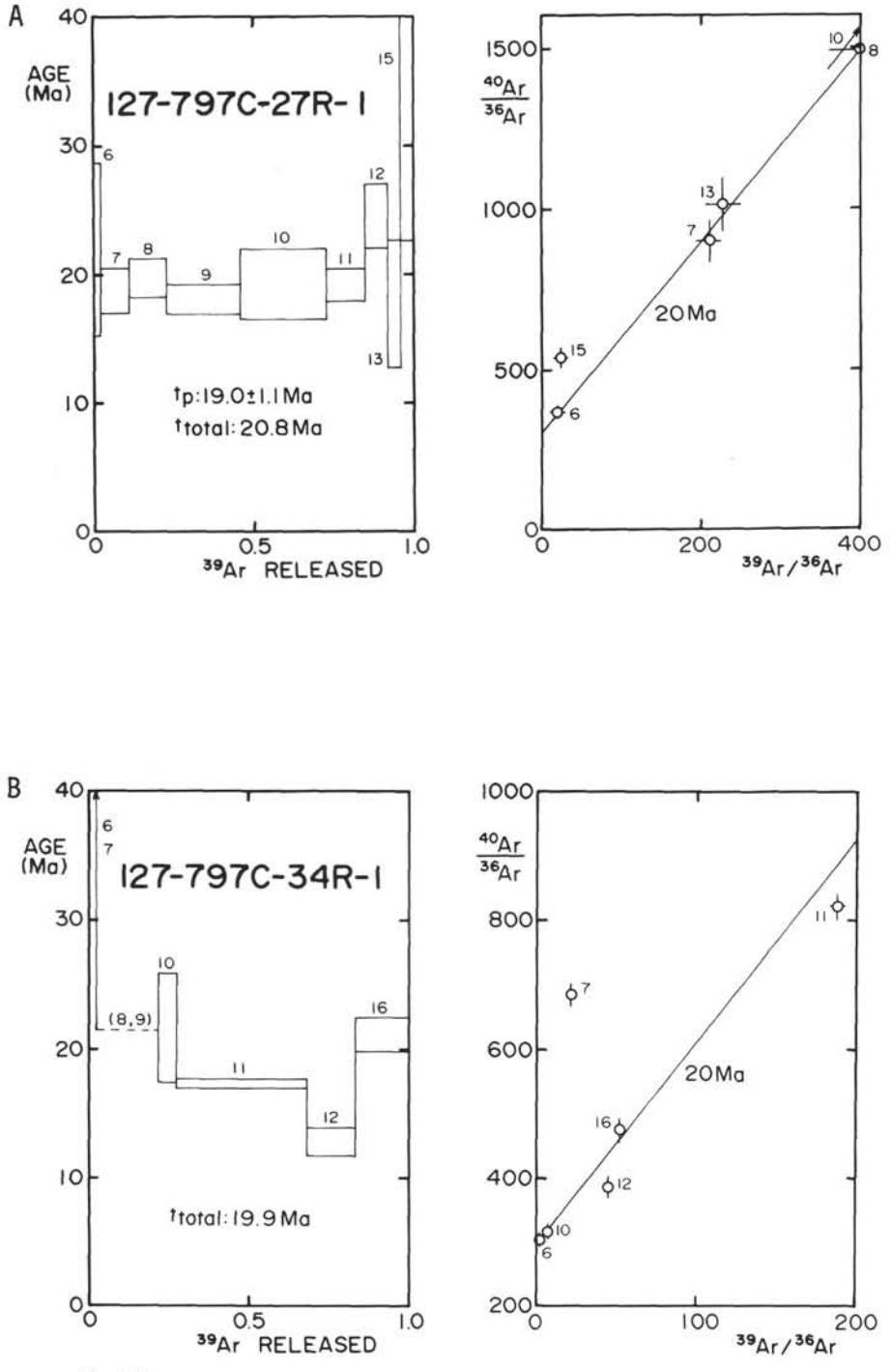

Figure 2. ^{40}Ar-^{39}Ar age spectra and isochron plots for samples from Sites 794, 795, and 797. The columns in the left-hand plots and the data points in the right-hand plots are labeled for the degassing temperature in 100°C. Uncertainty is indicated by 1σ. t_p: ^{40}Ar-^{39}Ar plateau age, t_{total}: ^{40}Ar-^{39}Ar total age. Temperature fractions in parentheses were lost and a degassing rate of 10% was assumed for ^{39}Ar. t_p values in parentheses indicate a pseudo-plateau age. The line in each isochron plot is a reference isochron. **A.** Aphyric basalt. **B.** Aphyric basalt. **C.** Sparsely plagioclase phyric basalt. **D.** Aphyric dolerite. **E.** Plagioclase-pyroxene phyric leucocratic dolerite. **F.** Phyric dolerite. **G.** Aphyric dolerite. **H.** Aphyric basalt. **I.** Aphyric dolerite. **J.** Silicified plagioclase phyric basalt. **K.** Sparsely pyroxene-plagioclase phyric basalt. **L.** Sparsely pyroxene-plagioclase phyric basalt.

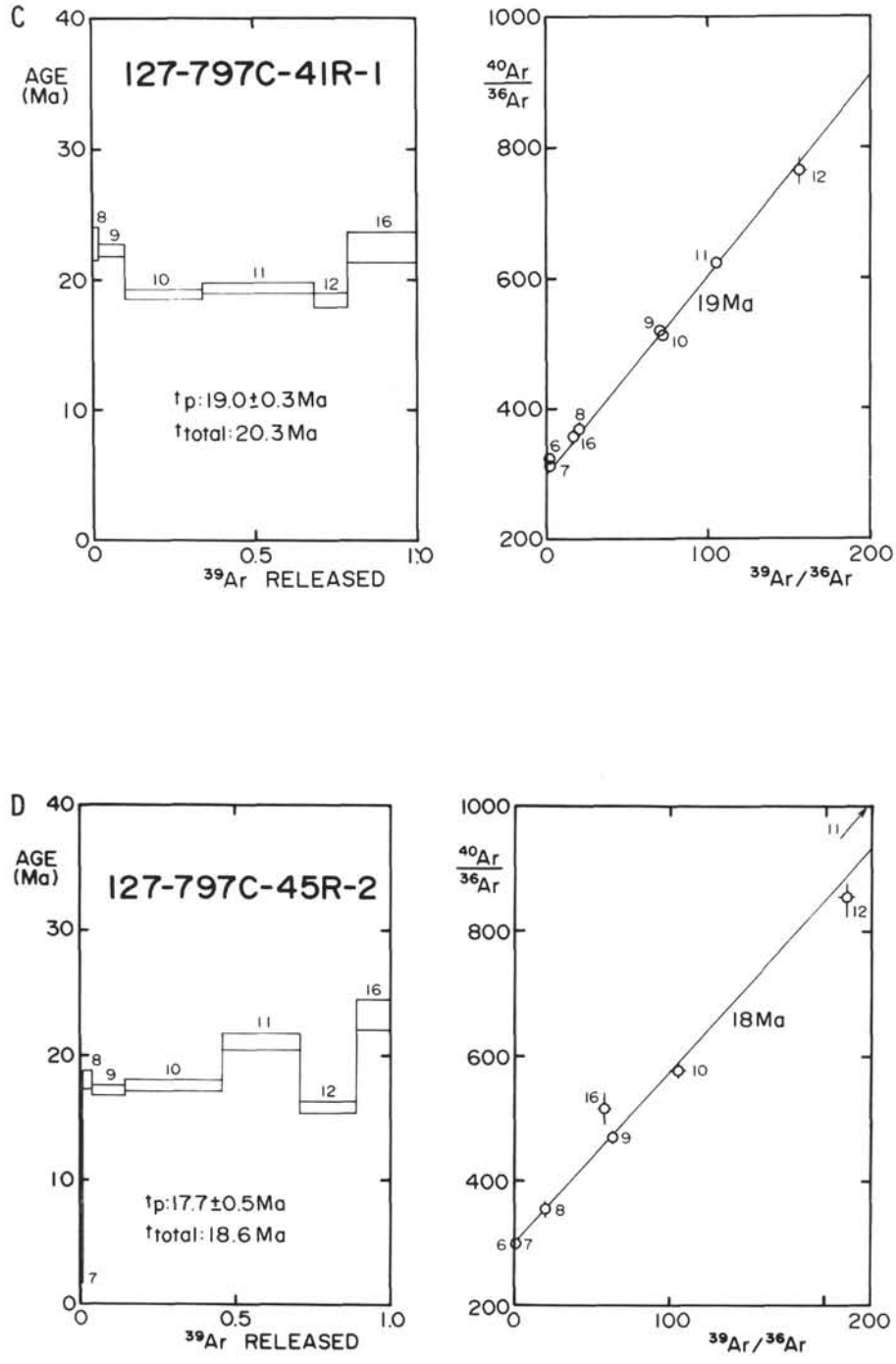

Figure 2 (continued).

However, we are not sure whether these estimates represent the age of formation. It is more conservative to say that such lower values represent the younger limits for the formation age of these samples.

Constraints on the Time of Volcanic Activity in the Japan Sea

The present ^{40}Ar-^{39}Ar analyses indicate that plateau ages range from 17.7 to 21.2 Ma, but are concentrated at about 19–21 Ma (Fig. 3).

For the three sites where basement volcanic rocks were recovered during Legs 127 and 128, no large differences exist in the ages obtained as a whole, but slight differences seem to occur among them. In the case of samples from Site 797, their ^{40}Ar-^{39}Ar plateau ages are concentrated at about 18–19 Ma. However, the apparent values do not reflect the stratigraphic order of the core samples recovered from the site, as shown in Figure 3. As mentioned previously, numerous intrusive rocks were observed in the core samples (Tamaki, Pisciotto, Allan, et al., 1990).

Most of the samples from Holes 794C, 794D, and 797C analyzed in this study are regarded as sills, whereas those from Hole 795B are lava flows. Hence, the younger ages of about 18 Ma may correspond to the time(s) of later intrusion of the sills. Because the ages for

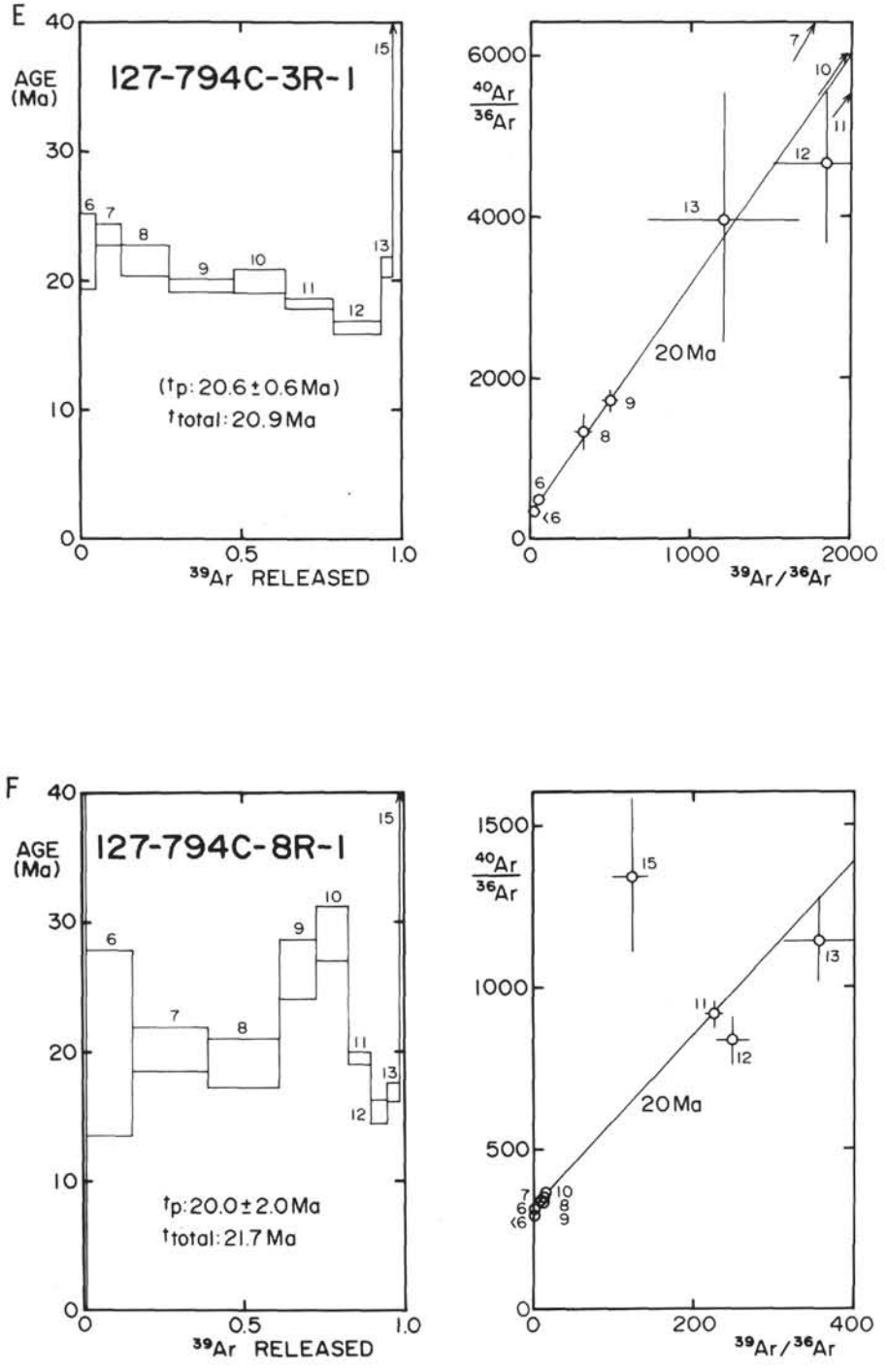

Figure 2 (continued).

samples from the upper part of Site 797 have not been determined because of low K content (Yamashita and Fujii, this volume), we cannot preclude the possibility that younger volcanic activity formed the basement of the Yamato Basin. From the age results for samples at Site 797, it can be concluded that the formation of the Yamato Basin had started by at least 19 Ma.

On the other hand, the samples from Site 794 show ages with a relatively narrow range of 20–21 Ma. Taking into account the experimental uncertainties of about 0.5–1 Ma, the ages obtained cannot be separated from one another. Although chemical differences have been observed between the upper part and the lower part of the drilled section at Site 794 (Ingle, Suyehiro, von Breymann, et al., 1990), the present results suggest that the time interval between them would not exceed 1–2 m.y. at most. Thus, based on these results from the Site 794 samples, it is inferred that the formation of the Yamato Basin would have been initiated by at least 20 Ma.

Further, the results from the samples from Site 795 could constrain the period of volcanic activity in the Japan Basin. As discussed previously, however, the samples do not show good plateau patterns. Hence, it is more conservative to say that the volcanic activities occurred at least within a range of about 15–25 Ma in the Japan Basin area.

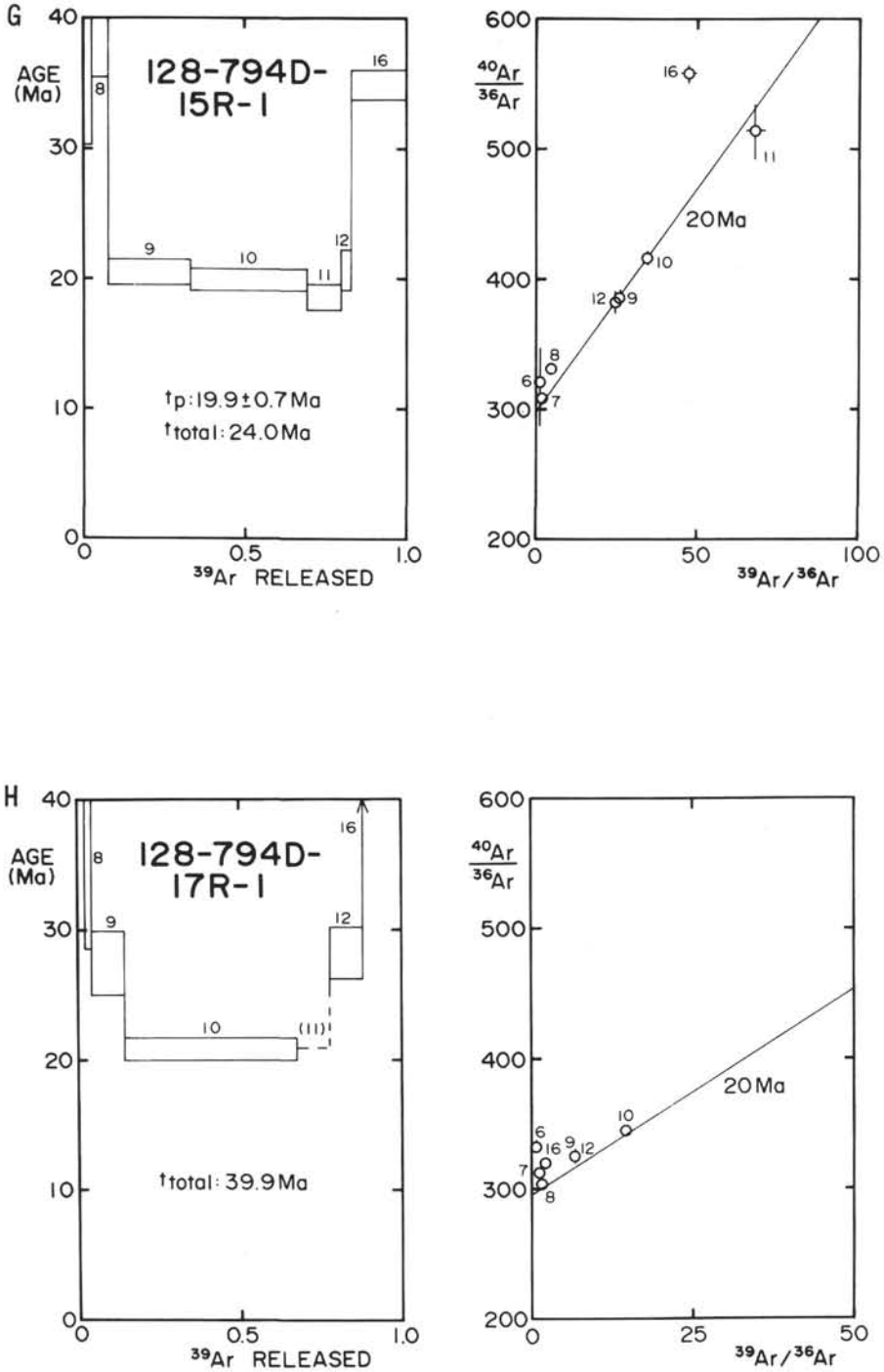

Figure 2 (continued).

In Figure 4, the present results are plotted together with radiometric age data for igneous rocks dredged from the Japan Sea floor (Kaneoka, 1990). The present results fit well within the age range estimated for the opening of the Japan Sea (more than 17 Ma and less than about 25 Ma). Such an age range has been inferred from radiometric age data compiled for dredged rocks in which the reliability of the data was evaluated carefully, including the effect of seawater alteration, the occurrence of excess Ar, and the identification of representative samples for the site concerned (Kaneoka, 1990; Kaneoka et al., 1990). Although the ^{40}Ar-^{39} Ar age data for dredged rocks from the Yamato Seamounts in the Yamato Basin (Kaneoka et al., 1990) give a significant constraint for inference, the present age data give a more precise constraint: that the volcanic activity forming the Yamato Basin started by at least 20 Ma. The formation of the Japan Basin might have been initiated slightly earlier, and we cannot deny the possibility that it might have already started by about 24 Ma.

As shown in Figure 4, there are no large age gaps between the radiometric age data for the samples from Legs 127 and 128 and those from the dredged samples recovered mostly from seamounts. This implies that the volcanic activity continued even after the formation of the Japan Sea floor for more than 5–10 m.y., though its intensity may have changed with time.

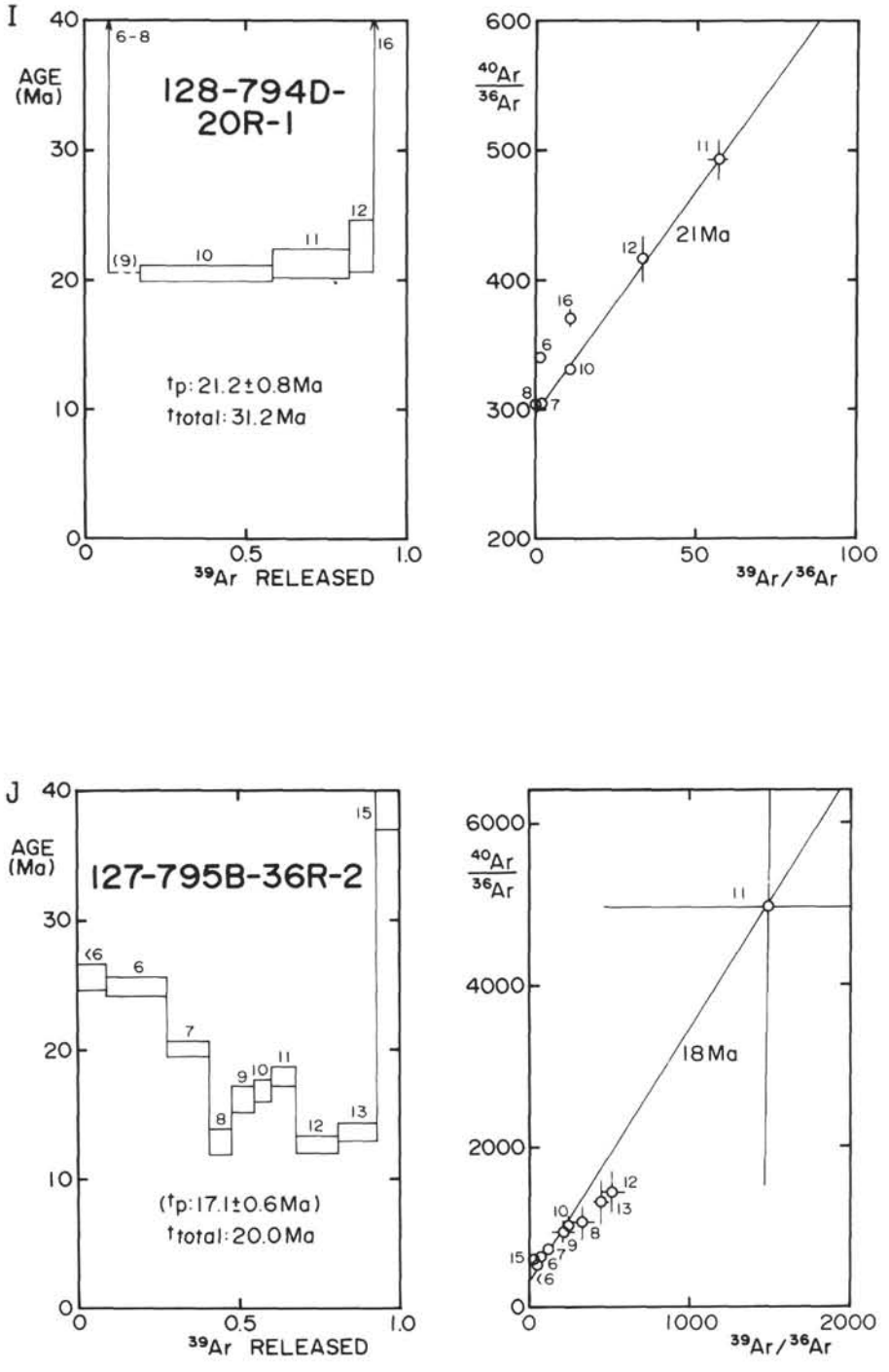

Figure 2 (continued).

When all the available age data are considered, there is no concentration at about 15 Ma, which might have been expected from inference based on shore-based paleomagnetic data (e.g., Otofuji et al., 1985). Much data have been accumulated from samples from the Yamato Basin area. Hence, if the 15-Ma event had occurred, it would have been related to the volcanic activity in the Japan Basin area. In light of this connection, to constrain the evolutionary history of the Japan Sea further, recovery of basement igneous rocks from the central part of the Japan Basin is essential. Then the evolutionary history of the Japan Sea may be clarified in more detail.

ACKNOWLEDGMENTS

We are grateful to the shipboard scientific parties of Legs 127 and 128 and the Ocean Drilling Program for supplying us with the samples used in this study. The samples from Hole 794D were courteously shared from samples prepared for paleomagnetic studies by Prof. Y. Hamano and the ODP Curator, to whom we express our sincere thanks. We also appreciate the staffs of JMTR at Tohoku University and the Isotope Center of the University of Tokyo for their help in irradiating and treating the samples. The manuscript was much im-

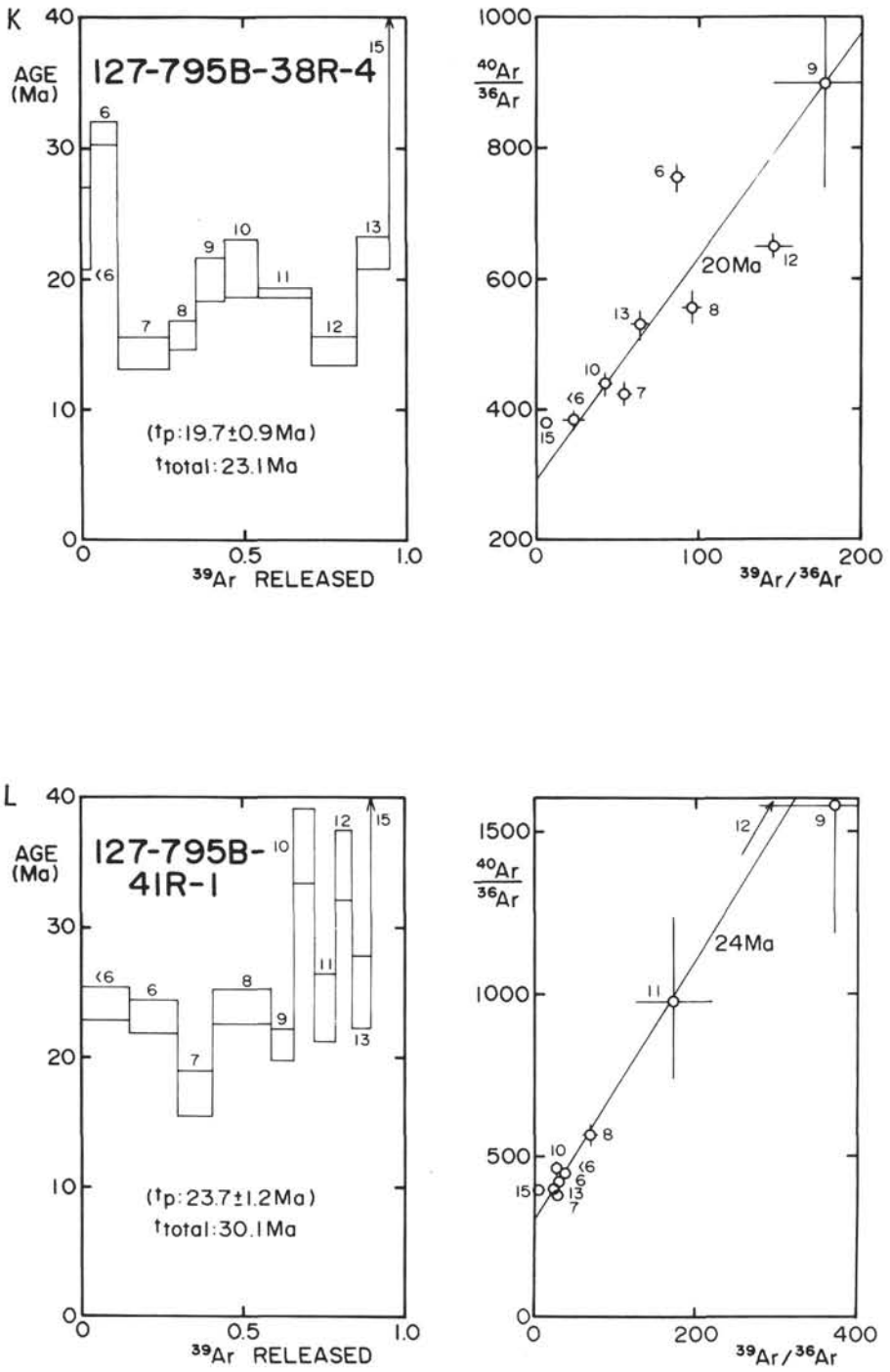

Figure 2 (continued).

proved by careful reviews and comments by Drs. R. A. Duncan and M. Pingle. The revised manuscript was prepared with the assistance of Mrs. K. Kudo, to whom we also express our thanks.

This study was financially supported in part by a Grant-in-Aid for Scientific Research (no. 02554028) to I. K. by the Ministry of Education, Science and Culture, Japan.

REFERENCES

Ingle, J. C., Jr., Suyehiro, K., von Breymann, M. T., et al., 1990. *Proc. ODP, Init. Repts.*, 128: College Station, TX (Ocean Drilling Program).

Isezaki, N., 1986. A magnetic anomaly map of the Japan Sea. *J. Geomagn. Geoelectr.*, 38:403–410.

Kaneoka, I., 1986. Constraints on the time of the evolution of the Japan Sea floor based on radiometric ages. *J. Geomagn. Geoelectr.*, 38:475–485.

———, 1990. Radiometric age and Sr isotope characteristics of volcanic rocks from the Japan Sea floor. *Geochem. J.*, 24:7–19.

Kaneoka, I., Notsu, K., Takigami, Y., Fujioka, K., and Sakai, H., 1990. Constraints on the evolution of the Japan Sea based on ^{40}Ar-^{39} Ar ages and Sr isotopic ratios for volcanic rocks of the Yamato Seamount chain. *Earth Planet. Sci. Lett.*, 97:211–225.

Lallemand, S., and Jolivet, L., 1985. Japan Sea: a pull-apart basin? *Earth Planet. Sci. Lett.*, 76:375–389.

Otofuji, Y., Matsuda, T., and Nohda, S., 1985. Paleomagnetic evidence of the Miocene counter-clockwise rotation of northeast Japan-rifting process of the Japan arc. *Earth Planet. Sci. Lett.,* 75:265–277.

Takaoka, N., 1976. A low-blank, metal system for rare-gas analysis. *Mass Spectr.,* 24:73–86.

Takigami, Y., Nishijima, T., Koike, T., and Okuma, K., 1964. Application of quadrupole mass spectrometer to the ^{40}Ar-^{39}Ar geochronological study. *Mass Spectra,* 32:227–233. (in Japanese with English abstract)

Tamaki, K., 1986. Age estimation of the Japan Sea on the basis of stratigraphy, basement depth, and heat flow data. *J. Geomagn. Geoelectr.,* 38:427–446.

Tamaki, K., Pisciotto, K., Allan, J., et al., 1990. *Proc. ODP, Init. Repts.,* 127: College Station, TX (Ocean Drilling Program).

Date of initial receipt: 18 March 1991
Date of acceptance: 4 February 1992
Ms 127/128B-200

Table 2. Summary of ^{40}Ar-^{39}Ar ages of samples recovered from the Japan Sea floor, Legs 127 and 128.

Core, section, interval (cm)	Rock type	^{40}Ar-^{39}Ar age (Ma) Total	Plateau (1σ)	Plateau temperature range (°C)	Integrated ^{39}Ar (%)
127-797C-					
21R-5, 105–107	Aphyric dolerite	20.4 ± 15.3	–	–	–
27R-1, 40–42	Aphyric basalt	20.8 ± 2.6	19.0 ± 1.1	700–1100	84.1
34R-1, 18–21	Aphyric basalt	[a]19.9 ± 1.1	–	–	–
41R-1, 7–10	Sparsely plagioclase phyric basalt	20.3 ± 0.6	19.0 ± 0.3	1000–1200	68.8
45R-2, 52–55	Aphyric dolerite	18.6 ± 0.5	17.7 ± 0.5	800–1000	44.8
127-794C-					
3R-1, 122–124	Plagioclase-pyroxene phyric leucocratic dolerite	20.9 ± 1.1	(20.6 ± 0.6)	(800–1000)	(50.6)
8R-1, 6–8	Aphyric dolerite	21.7 ± 3.0	20.0 ± 2.0	600–800	60.9
128-794D-					
15R-1, 73–75	Aphyric dolerite	24.0 ± 1.3	19.9 ± 0.7	900–1200	76.0
17R-1, 81–83	Aphyric basalt	[a]31.9 ± 2.0	–	–	–
20R-1, 17–19	Aphyric dolerite	[a]31.2 ± 2.1	21.2 ± 0.8	1000–1200	72.7
127-795B-					
36R-2, 85–88	Silicified plagioclase phyric basalt	20.0 ± 0.9	(17.1 ± 0.6)	(900–1100)	(20.2)
38R-4, 90–93	Sparsely pyroxene-plagioclase phyric basalt	23.1 ± 1.6	(19.7 ± 0.9)	(900–1100)	(35.4)
41R-1, 90–93	Sparsely pyroxene-plagioclase phyric basalt	30.1 ± 2.2	(23.7 ± 1.2)	(<600–600)	(30.2)

Note: Values in parentheses are less reliable because of the small proportion of total ^{39}Ar represented by these steps or because of the possible redistributed nature of the Ar isotopes during neutron irradiation.
[a]Calculated excluding the temperature fractions for which the extracted Ar gases were lost.

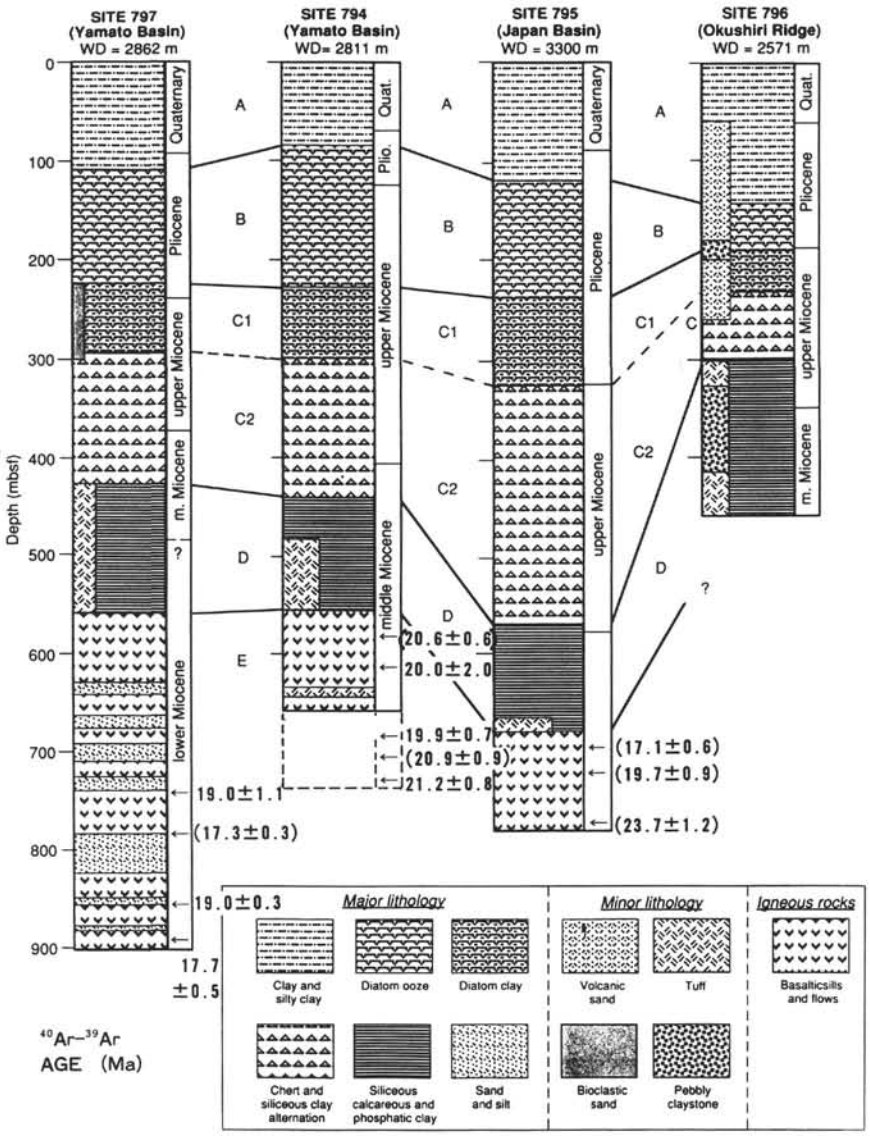

Figure 3. Leg 127 lithologic columns and results of ^{40}Ar-^{39}Ar ages. The samples recovered at Site 794 during Leg 128 are shown by extending the column to indicate the relative recovered depths. The ages in parentheses are less reliable. The lithofacies are after Tamaki, Pisciotto, Allan, et al. (1990).

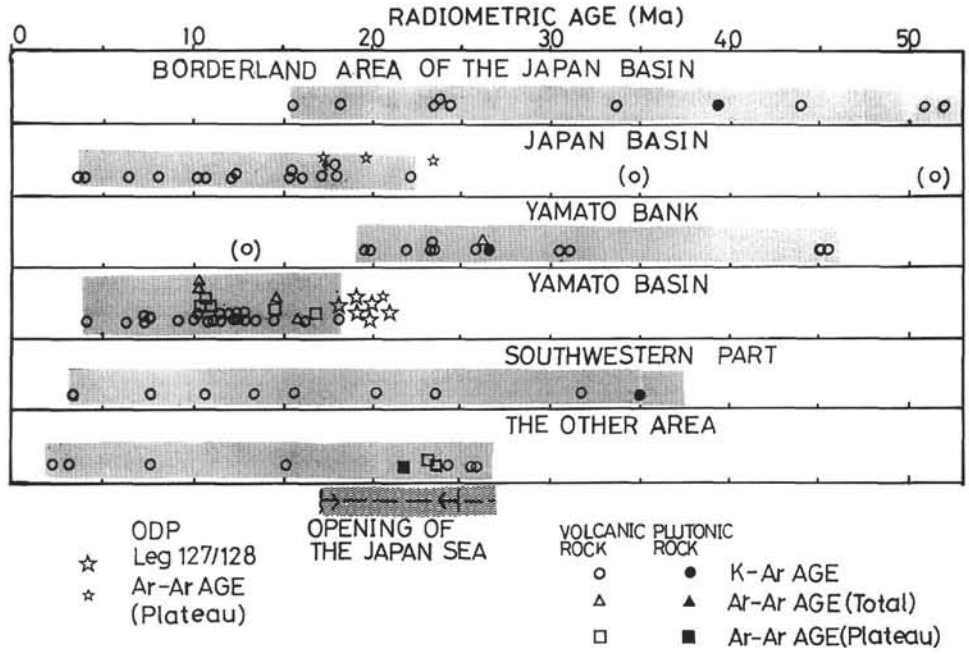

Figure 4. Radiometric age data for igneous rocks recovered from the Japan Sea floor. The samples from Legs 127 and 128 were recovered by drilling, the other samples were recovered by dredging. The smaller symbol for Legs 127 and 128 indicates less reliable data. "The other area" includes the Japan Sea borderland along the Japanese Islands. The results from Legs 127 and 128 refine the period estimated previously for the opening of the Japan Sea (Kaneoka, 1990; Kaneoka et al., 1990).